HYDROGEN CRACK RESEARCH IN WELDED JOINTS WITH ACOUSTIC EMISSION AND IMPLANT TEST

Roberta A.L. Vieira, roberta_adrielle15@hotmail.com[1]
Waldemir dos P. Martins, waldemir@ifma.edu.br[1]
Valdemar S. Leal, valdemar@ifma.edu.br[1]
Antônio E. Macedo Paiva, ernandes@ifma.edu.br
Victor H.B Santos, victor.hbs@hotmail.com[1]

[1]IFMA – Instituto Federal do Maranhão/Campus Monte Castelo, Av. Getúlio Vargas, 04. Monte Castelo. CEP:65030-005. São Luís/MA.

Abstract. *There were an increase in the need for steel which is used to transport fluids such as oil and natural gas due to the discovery of new reserves in harsh environments and reserves distant from consumption centers, so it enhanced progressively the demand for high- strength steels and lower costs. Therefore, HSLA steels (high strength, low alloy) have been used because of its good weldability, mechanical strength and lower cost due to the fact that thinner plates can be used. However, these steels tend to have weldability problems due to the hydrogen cracks (HC). The aim of this study was to investigate the relationship between heat input variation and the origin of HC, with gas and without purge gas, using implant test coupled to an acoustic emission system in order to define the moment of crack formation and its propagation. The welding process used was the FCAW-S and as the filler metal it was used a self-shielded tubular wire E71T-11. In this study, it was possible to verify the influence of the use of shielding gas and welding energy in the formation of the microstructure and development of crack in the material of study, demonstrating the efficiency of the AE technique in the verification of HC.*

Keywords*: HSLA steel, hydrogen cracks, acoustic emission, implant test, purge gas.*

1. INTRODUCTION

Due to the great technological advance and increase of oil and natural gas production, the high-strength low alloy steel (HSLA) is being widely used for economic reasons. The use of pipes made of steels with better mechanical properties and weldability has contributed to the production of oil and gas pipelines with lower costs. So, it reduces the thickness of the pipes, maintaining the working pressure, and consequently reducing the weight; also, it becomes easier for assembly and it is necessary a less amount of filler metal and other welding consumables (Aquino, 2011; Pereira et al, 2012).

One of the big metallurgical problems that may happen to welded HSLA steels is the hydrogen cracks. These cracks form in the welded joints of this material and occur due to the fusion welding process, which generates thermal cycling. So, it causes changes in the stress state, microstructure and properties in the fusion zone (FZ) and in the heat affected zone (HAZ). During the cooling process, the austenitized regions undergo granulometric changes and there are transformations in different components according to the cooling rate of the weld material. (Fals, Trevisan, 1999; Martins, 2013).

The introduction of hydrogen (H) during the welding of HSLA steels results in the formation of hydrogen cracks, also known as cold cracks (Soeiro et al., 2013). According to Bezerra (2005) and Nevasmaa (2013), this type of cracks is a serious problem in welding of high strength and it refers to the loss of ductility of the material, so it develops cracks. The beginning and propagation of these cracks occur in hours, or even days, after the welding. For the formation of this type of crack, the main factors are: hydrogen concentration in the joint, metal microstructure, residual stress level and weld cooling temperature between 150 ° C and -100 ° C (Nevasmaa, 2013). In order to analyze the susceptibility of a material for the formation of such crack when welded, the use of developed tests has facilitated the evaluation of welding procedures, providing welds free or with negligible amounts of cold cracks (Bezerra, 2005). The tests developed to evaluate the susceptibility of the material to cold cracking of welded joints are classified as direct and indirect. The main types of direct tests (where the stresses originate from the assembly itself) are: Controlled Thermal Severity (CTS), Tekken (Y-Groove Restraint Test), LEHIGH constraint test and G-BOP test. These tests allow a quick assessment of the joint (FZ and HAZ) by counting the number of cracks for each specimen (SM).

The indirect ones (the stress come from an external device) can be pointed out: Implant, TRC (Tensile Restraint Cracking), RRC (Rigid Restraint Cracking), ASC (Augmented Strain Cracking) and CLR (Constant Load Rupture). These tests are performed on specimens where they are subjected to a load controlled by an external device (Boellinghaus, Viyanit, Zimmer, 2010).

The Implant test, used in this study, is an external constraint test that combines characteristics of both methods. Most of the external constraint tests have been established for the hydrogen cracks to occur in the heat affected zone (HAZ). In the indirect tests, it is determined the highest level of stress that can be applied without occurring the crack formation in a specimen, known as the critical stress, characterizing the susceptibility in the evaluated region (Silva, Ferraresi, 2006).

However, only the use of existing susceptibility tests does not guarantee that their responses will be used for a practical application. Thus, it is necessary to use other testing devices for more information. An alternative have been used, it is called technique of Acoustic Emission (AE) (Martins, 2013). This technique has been widely in recent decades used due to its versatility, low cost and ability to monitor phenomena in real time. Its monitoring is done based on the generation of acoustic emission waves to detect the instant of formation and propagation of the crack (Ferraresi, 1996; Fals, Trevisan, 1999). Therefore, in order to obtain more precise results on the formation and propagation of hydrogen cracks, the aim of this work is to present a study, using an Acoustic Emission system coupled in the Implant test, in order to determine the hydrogen cracking behavior of the weld joint with and without purge gas.

2. EXPERIMENTAL PROCEDURE

2.1. Materials, equipments e methods

The test plates (implant placement plate) and the implants were removed from a API X80 steel plate with dimensions of 330 mm x 200 mm x 20 mm (length x width x thickness). The chemical composition and mechanical properties of the material are given in Tab. (1). The implants were removed in the direction of lamination and prepared according to AFNOR NF A 89-90, and the implants welding were prepared in the same direction. The reason for the use of the same material for manufacturing of implants and test plates is because of the non-variation of the thermal conductivity. The test plate was machined for the removal of the surface oxide layer. Two equally spaced holes (2) of 6,35 mm and 2,5 mm of diameter were made for implant and thermocouple fixation (temperature monitoring of placement of AE sensor), which is shown in Fig. 1 (a); and the figure of the implant, with standardized dimensions, is shown in Fig. 1 (b).

Table 1. Chemical composition and mechanical properties of the steel.

Chemical Composition (wt %)								
C	**Mn**	**Si**	**Nb**	**V**	**Ti**	**Cr**	**S**	**Al**
0.05	1.81	0.29	0.069	0.033	0.02	0.17	0.001	0.02
Cu	**Ni**	**Mo**	**Sn**	**P**	**B**	**Ca**	**As**	**N**
0.02	0.01	0.21	0.001	0.017	0.0002	0.0012	0.003	0.0034

Mechanical Properties					
YS (Mpa)	**TS (MPa)**	**ε (%)**	**Hv**	**CE (Pcm)**	**CE (IIW)**
550-660	631-741	26	225-250	0.18	0.44

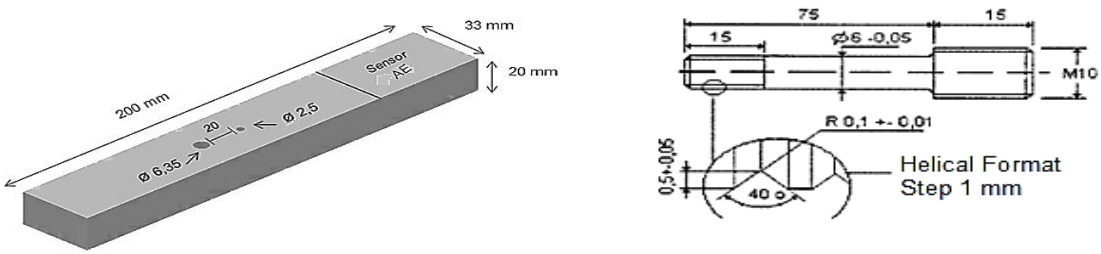

(a) **(b)**

Figure 1. (a) Schematic Representation the plate with the roles for placement of implant and thermocouple. (b) Size of the implant according to AFNOR NF A89-100.

The self- shielded tubular wire of diameter 1.6 mm (E71T-11) was used as filler metal. The chemical composition and mechanical properties of the filler metal are shown in Tab (2). The carbon equivalent was determined by Eq. (1) of Ito-Bessyo and (2) of IIW (International Institute of Welding) and they are shown in Tab. (1) and (2).

$$\mathbf{CE\ (P_{cm}) = C + Si/30 + Mn/20 + Cu/20 + Ni/60 + Cr/20 + Mo/15 + V/10 + 5B} \quad (1)$$

$$\mathbf{CE\ (IIW) = C + Mn/6 + (Cr + Mo + V)/5 + (Ni + Cu)/15} \quad (2)$$

Equation (1) is known as the carbon equivalent parameter, crack measurement parameter or Ito-Bessyo formula. This is used for steel with carbon content below 0.12%; and a CE (PCM) value ≤ 0.25% is recommended for better weldability results and minimizing cracking. Equation (2) is known as the carbon equivalent formula of IIW. It is used for steels with high carbon content (C > 0.12%), and it is widely used in the industry due to its wide applicability CE (IIW) values ≤ 0.45% indicate good weldability of steels.

Table 2. Chemical composition and mechanical properties of self- shielded tubular wire E71T-11.

Chemical Composition (wt %)				Mechanical properties			
C	**Mn**	**Si**	**Al**	**YS (MPa)**	**TS (MPa)**	**ε (%)**	**CE (Pcm)** 0.29 **CE (IIW)** 0.36
0.25	0.7	0.4	1.6	500	630	23	

2.2. Acoustic Emission System- AES

In order to analyze the signals of the crack, an acoustic emission system (AES) was used. It is composed of a data acquisition board (A/D), sensor and computational interface, as shown in Fig. 2 (a). The data acquisition board converts the output signal from the wave rectifier circuit from its analog to digital form. The Measurement Computing Model 1208FS converter connects to the computer through a USB cable, that makes the data to be transmitted to the computer. The WD-FT64 crack detection sensor converts surface vibrations caused by an elastic wave into an electrical signal that will be processed by the AES (Martins, 2013).

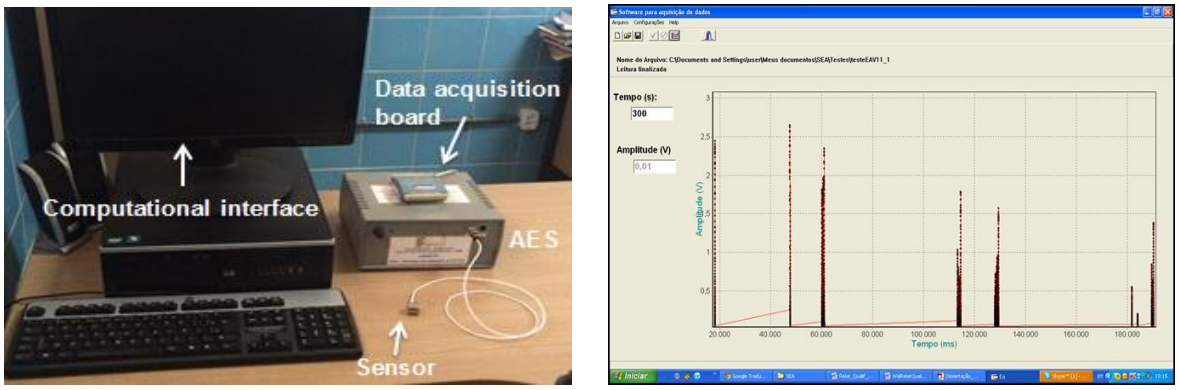

(a) **(b)**

Figure 2. (a) Equipment that forms the Acoustic Emission System - AES. (b) AE Signal Analyzer.

The Acoustic Emission Analyzer is the computational program, as shown in Fig. 2 (b), which was developed specifically for this system, that was used to capture and store the data with a previously established drop of the signal. Thus, the computer only stores the data related to the propagation of the cracks and ignoring the noises. The system works in the range 0 to 10 V and the noise drop, after preliminary tests, based on the methodology adopted by Martins (2013), was 0.32 V. The acquisition rate was 2000 points/s for all specimen; and the recorded signals were at a minimum of 0.32 V, it means that it was over the noise level of the acoustic emission system. Figure 2 (b) shows the signs of AE obtained by the AES.

2.3. Implant Test

To perform the tests an equipment was used for the implant test; it has the purpose to apply a load to the implant and to impose the tension condition. The equipment used is composed of two types of systems: a traction system (composed of a hydraulic system) and a monitoring system. Its functions are based on traction of the specimen; so, it simulates a state of internal stress in welded joints, it monitors the relief of stresses and the eventual occurrence of cracking (or rupture of the implant). Figure 3 (a) shows the LTPSolda / DMM / IFMA welding laboratory implant test equipment. The test is based on inserting the Implant into a hole in the top of the test equipment attached to the holder

by threading and then to the plate with the hole. After its positioning in the hole of the plate, the notched part of the implant is leveled with its surface. After this assembly, a 100 mm soldering pass was made on the plate passing over the hole and the SM. The tests were performed under predetermined conditions using the welding process and the chosen consumable. The welds were performed with and without purge gas, and the argon was used as the purge gas in the low rate of 2 l/min. The purge gas was injected during welding and it remained in the welded joint until it reached room temperature. Figure 3 (b) schematically shows the implant test with the purge gas inlet.

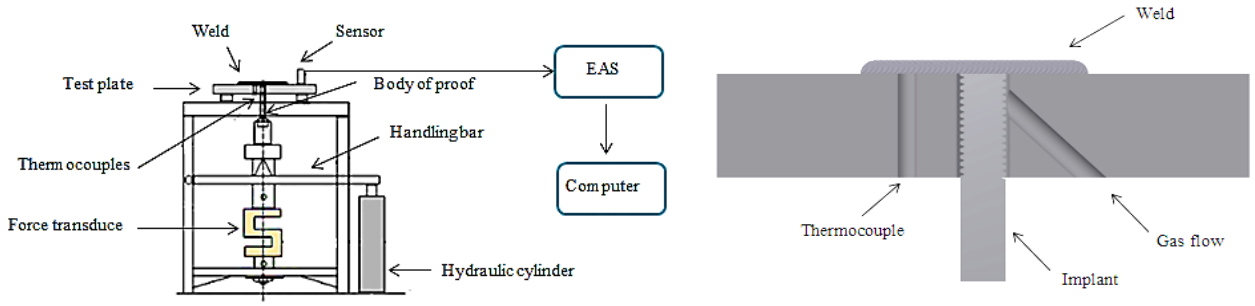

(a) **(b)**

Figure 3. (a) Implant equipment test LTPSolda/DMM/IFMA. b) Test plate for tests using purge gas.

Before the tests, the plate and the implant were cleaned with acetone. After the welding process and before the complete cooling of the solder at a temperature of 150° (measured from the thermocouple installed in a hole near to HAZ), the load was removed from the hydraulic system, and then the traction was gradually applied on the implant. In this way the SM started to be submitted to a pure effort of constant traction throughout the test. The constant tensile load was measured from the TSA load cell, Fig.4 (a). It has strain gage, sensitive to variations in applied force and capable of transforming mechanical stresses into electrical signals and potential to measure up to five tons. The weighing transmitter received the signal from the load cell and transmitted it to the analog/digital interface, showing the intensity of the request at a given instant through means of a digital indicator, Fig.4 (b).

(a) **(b)**

Figure 4. (a) Force transducer TSA Model. (b) Weighing transmitter.

When the solder reached the desired temperature, the AE sensor was placed on the test plate, and then the signal acquisition was started for 24 hours or until the implant rupture.

2.4. Analysis of the specimens

The implants tested were analyzed with the results presented by the AES. From the obtained signals, it was possible to prove the existence of the crack; and from the result of the acquisition of the acoustic emission sensor was possible to verify the feasibility of AE in the detection of hydrogen cracks. In this way, it was possible to relate the results of the acquisition of the acoustic emission sensor in the detection of hydrogen cracks. In this study, we considered welded implants with and without purge gas. The purpose of the purge gas is to verify its contribution in preventing the phenomenon of HC and / or its influence on the result during the occurrence of the phenomenon.

3. RESULTS AND DISCUSSIONS

In the Table (3) can be seen the results of tests with different energies welding and applied loads, where the variables related to the implant test are C and variables resulting from data acquired by the AES are t_{pi}, t_{pf}, v_p, n_p.

Where:
C – Load registered by the load cell in the implant (Kgf);
t_{pi} – Time of the first excitation (peak) recorded by the AES (ms);
t_{pf} – Final time registered by AES on break or not the specimen (ms);
v_p – value greater arousal (maximum amplitude) registered by the AES (V);
n_p – Number of excitations (peaks) stored above the cutoff limit throughout the test.

Table 3. Results of AE.

Test	Condition	E (Kj/mm)	C (Kgf)	t_{pi} (ms)	t_{pf} (ms)	v_p (V)	n_p	Result
I1	With purge gas	1.0	300	-	-	-	-	**NT**
I2		1.5	1120	511561	18891430	0.42	2	**TR**
I3	Without purge gas	1.0	1000	10010	10190	0.92	2	**TR**
I4		1.5	1120	1971450	1971458	0.49	1	**TR**

Symbols: E = Energy generated in arc welding; **Amb** = Ambient Temperature;; **NT** = Specimen not fractured and not presented signal in the AES; ; **TR** = Specimen that fractured and presented signal in the AES;

In Table 3 it can be observed that the I1 did not appear any crack, as evidenced by its micrograph, and also no signal registered in the AES. The low residual voltage due to the low load applied during the test can explain the non-crack appearance, despite the low welding energy. According to Martins (2013) a minimum load applied at the implant of about 1116 kgf is required to the cracking and/or rupture of the SM occur.

The I2 showed a crack, Fig. 5(a) and the signal capture by the AES, Fig. 5(b). After 8.53 min that the test started, the AES recorded the first peak of 0.35 V, indicating if the cracking occurred. After 314.86 min (5.25 h), the second peak was recorded with an amplitude of 0.42 V, indicating if it was the propagation of HC.

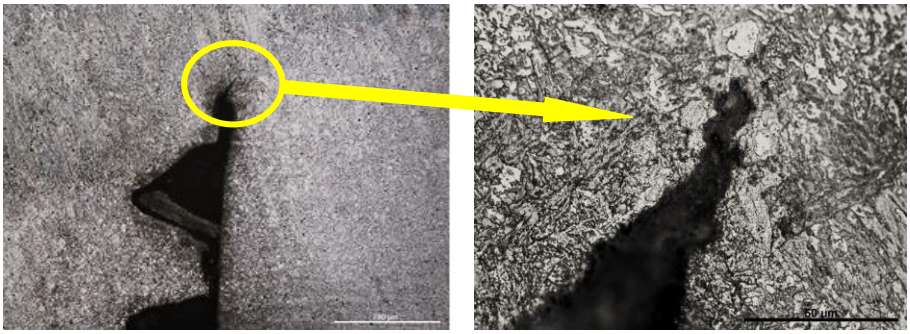

(a)

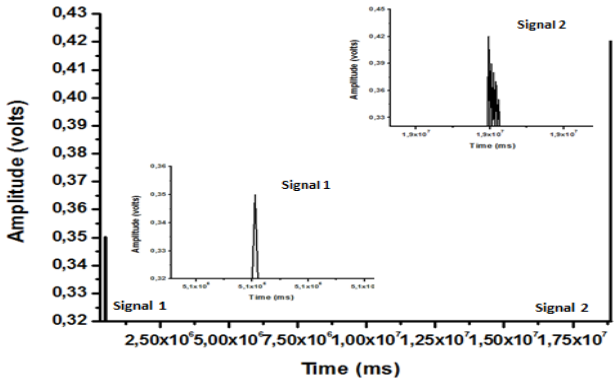

(b)

Figure 5. (a) Micrograph of the HC in the CGHAZ to I2. (b) Signal captured by AES for I2.

It is observed in Fig. 5(a) that the crack was generated in the boundary at the CGHAZ (region of the coarse grain HAZ)/FZ boundary, probably because of the presence of the restriction, crack propagation time, residual hydrogen from welding and the carbon equivalent content of the material found in the range of susceptible materials. This crack propagates without extending in the direction of the FZ, proving to be a HC. The crack is small possibly due to the low residual stress imposed by the weld.

In the welding of I3, purge gas was used to protect the fusion pool against atmospheric air and consequently the action of hydrogen, which is one of the causes of the onset of HC. The test I3 showed a crack, Fig. 6(a) and the signal capture by AES, Fig. 6(b). After 10 seconds that the test started, the AES recorded the first peak of 0.5 V with duration of 180 ms, indicating whether cracking was present. After 17.65 s, the second peak was recorded with amplitude of 0.92 V, indicating if it was the propagation of HC.

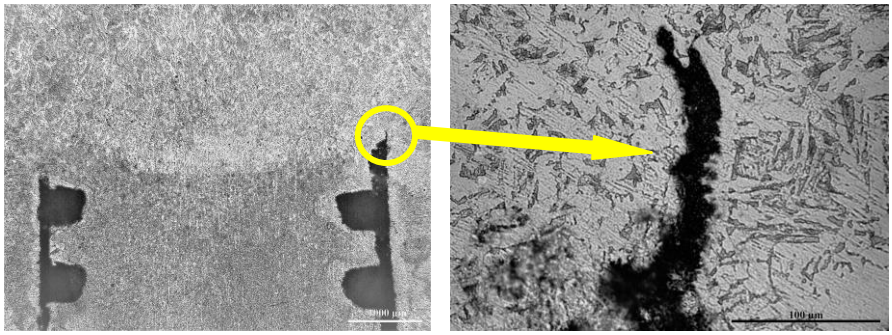

(a)

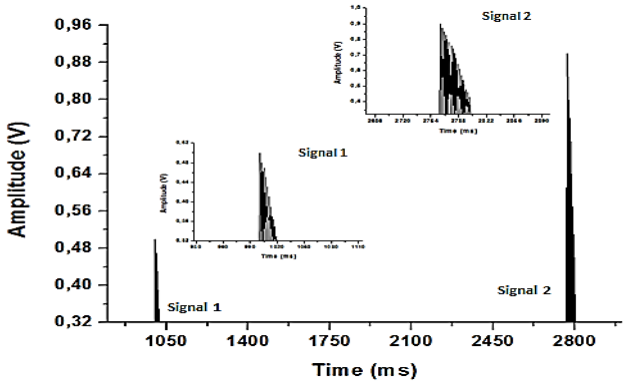

(b)

Figure 6. (a) Micrograph of the HC in the CGHAZ to I3. (b) Signal captured by AES for I3.

As occurred in I2, the crack formed at the test I3 also was placed at the CGHAZ / FZ boundary and it is justified as shown for the I2, differing in the formation of signals with larger size and amplitude in a shorter time interval, between the first and last peak, proving to be an HC. The crack appears with a slight indication that it would propagate in the direction of the FZ.

The I4, Fig. 7(a) was welded using the purge gas for the same purpose as the I3 test. Micrograph of the implant was performed and the appearance of cracking and signal capture in the AES was observed, Fig. 7(b). The peak appeared after 33 minutes of the beginning of the test with amplitude of 0.35 V and duration 18 ms, indicating if it is a micro crack of H. The behavior of the same is similar to the one of I3 already discussed.

From the preliminary analysis, it is concluded that the material used is susceptible to HC with the Implant test and the welding conditions imposed in this work. In the presence of purge gas and welding with self- shielded tubular wire, cracks occurred regardless of the welding energy, but always with applied load. The purge gas shielded the lower part of the implant; however, the face of the weld bead was unprotected because the shielding gas from the consumable itself was unsatisfactory. Therefore, the consumable contributed to the appearance of the crack. The presence of H can cause cracks in both HAZ and FZ with different orientations, as seen, in agreement with the literature.

Hydrogen cracking often originates from stress concentrators, such as at the edge or at the root of the weld. They can be micro or macroscopic, several centimeters long. HC occurs mainly in HAZ, in the grain growth region, but may also occur in the fusion zone. In this region, cracking has been observed more recently because of the use of steels with lower carbon equivalent, but with high mechanical strength that is greater than 590 MPa (60 kgf/ mm^2).

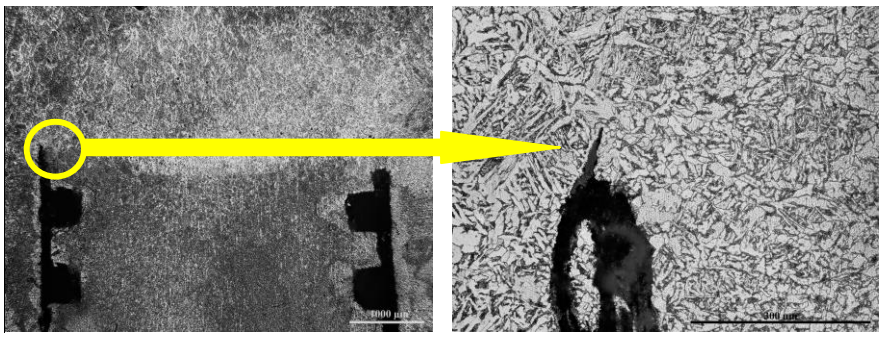

(a)

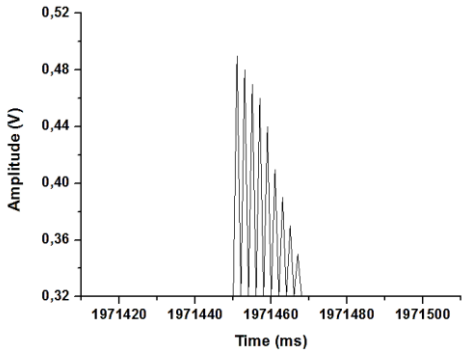

(b)

Figure 7. (a) Micrograph of the HC in the CGHAZ to I4. (b) Signal captured by AES for I4.

3.1 Microstructure

In Figure (8) is presented the BM (base metal) microstructures (implant and test plate) with different applications are presented. It is possible to observe a microstructure formed by Primary Ferrite (PF) which is attached in the matrix and Bainite (B) spread throughout this matrix. This microstructure resembles the same one worked by Martins (2013) in his work, which used material similar to that of this study.

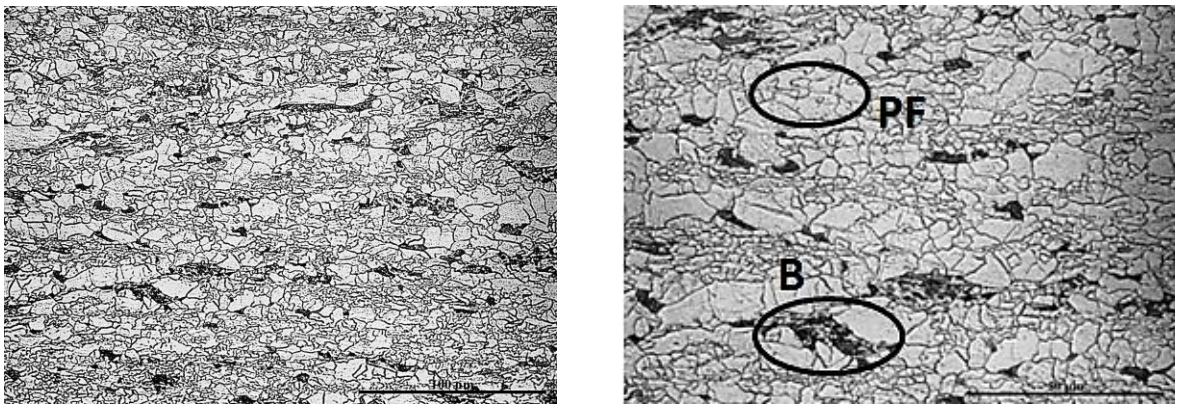

Figure 8. Micrograph of the BM. 750X and 1500X extension, respectively. 2% Nital.

Figure (9) shows the structural behavior of FZ and HAZ, respectively, for different welding energies used in the tests, with/without purge gas. In the HAZ, the coarse grain region (CGHAZ) is evaluated. The FZ microstructures of the tests show that regardless of the welding energy there is a formation of Grain boundary Ferrite PF(G), Acicular Ferrite (AF) and Ferrite with Aligned Second Phase FS(A), with higher incidence of PF(G) and FS(A) in the welding condition without purge gas (I1, I2). With the purge gas (I3, I4) there is a reduction of PF (G) and FS (A) and appearance of AF in a greater proportion. In the presence of the purge gas and with the variation of the welding energy a refinement of the microstructure (I3, I4) is observed.

FZ **HAZ**

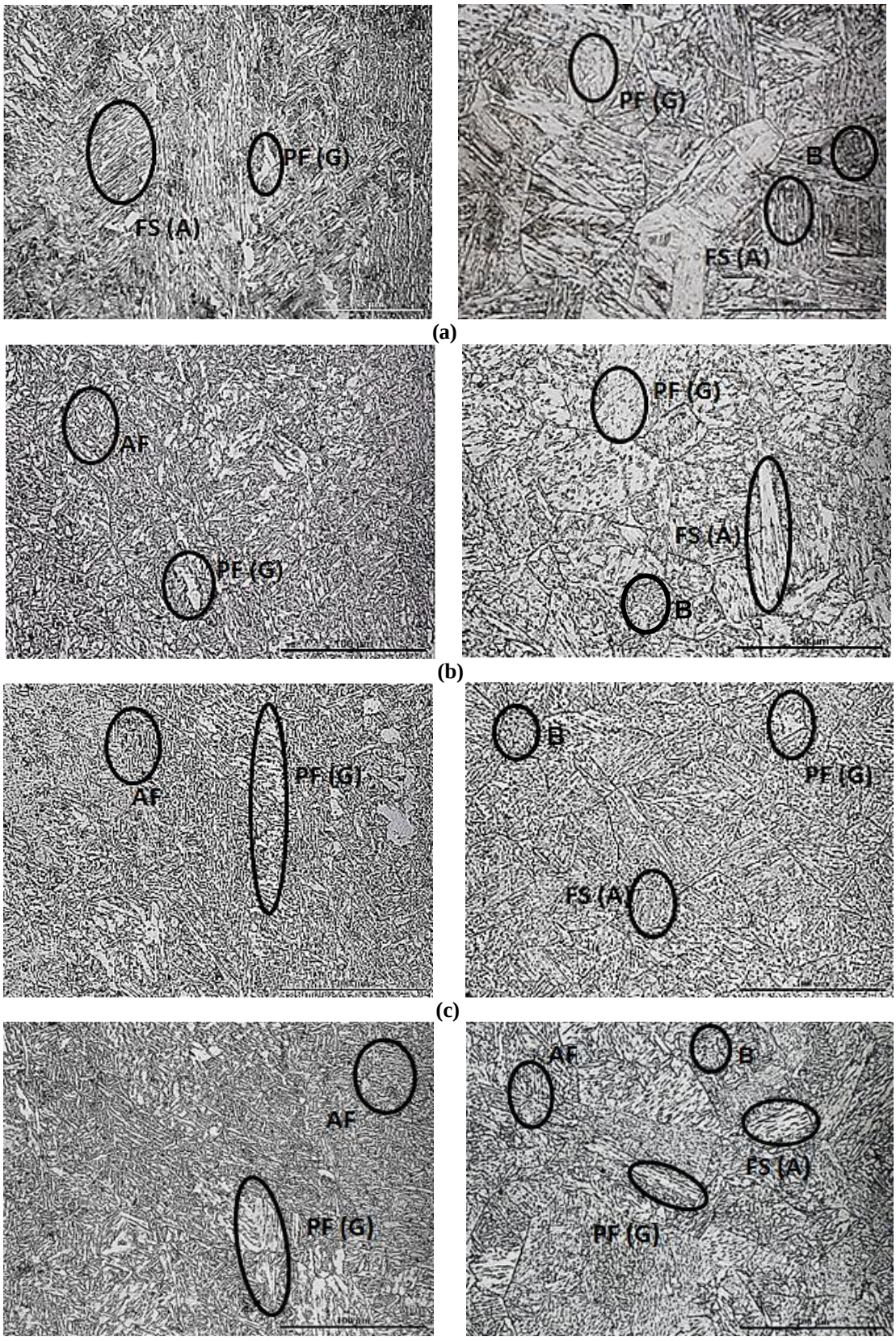

Figure 9. Micrograph of the FZ e HAZ, respectively: (a) I1 (1 kj/mm); (b) I2 (1.5 kj/mm); (c) I3 (1 kj/mm); (d) I4 (1.5 kj/mm).

The behavior of the microstructures of the CGHAZ are similar, even for different welding energies. However, a reduction of PF(G) and FS(A) and the refinement of the microstructure in the condition with purge gas which is possibly influencing. The increase in welding energy also contributed to the refinement of the microstructure. Although the PF(G) is not very fragile, it can help in the propagation of the crack of hydrogen, because it is a microconstituent that is usually among microstructures of greater resistance and greater fragility; it does not withstand the deformations due to the concentration of tension. The microconstituents formed in the HAZ are similar to the work of Martins (2013) that used base material and welding energies similar to the one in this study.

Analyzing the hydrogen cracking it can be affirmed that the self- shielded tubular wire used in this work did not promote, on its own, many microstructural changes, but it had an influence on the susceptibility of this type of crack. This is due to the presence of PF(G) and FS(A).

3.2 Microhardness

In Figure (10) are shown the average values of microhardness in FZ, CGHAZ and BM. This microhardness behavior shows, according to Tab. (4), that the hardness in CGHAZ is higher than in the other regions.

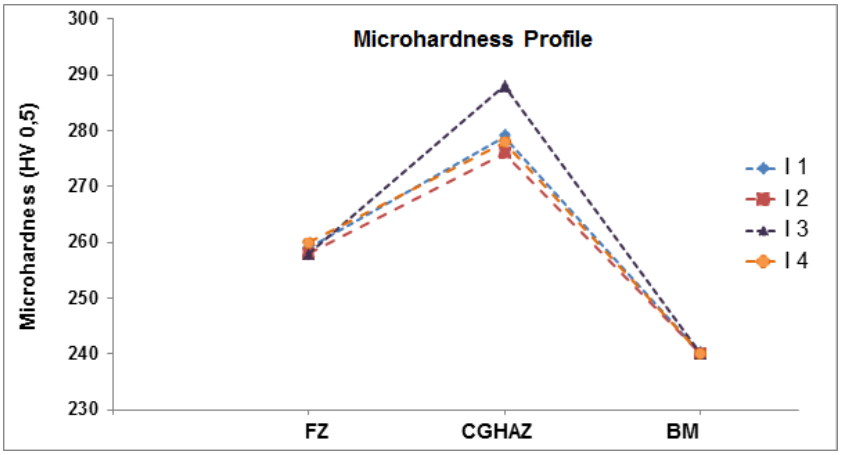

Figure 10. Microhardness Profile in different regions of the tests I1, I2, I3 e I4.

From the analysis of the microhardness behavior presented in the tests, a hardness rate in the CGHAZ is observed from 276Hv to 288Hv, in the FZ from 258Hv to 260Hv and in the BM without much variation of the order of 240 Hv. From the graph, a small degree of dispersion in the measurements is observed which attributed to structural heterogeneities, because of regions that are recrystallized or not.

Table 4. Microhardness values of the FZ, HAZ/CGHAZ e BM.

E (kj/mm)	Test	Zone	Points							Mean	Standard deviation
			1	2	3	4	5	6	7		
1.0	I1	FZ	258	256	265	259	264	261	252	259	4.5
		CGHAZ	276	279	302	278	288	283	268	279	10.8
1.5	I2	FZ	257	260	262	254	258	261	255	258	3.0
		CGHAZ	266	269	286	278	272	276	283	276	7.3
1.0	I3	FZ	257	260	255	256	260	258	261	258	2.3
		CGHAZ	267	288	292	304	288	281	309	288	14.0
1.5	I4	FZ	260	251	257	261	258	270	262	260	5.8
		CGHAZ	268	271	284	287	270	280	278	278	10.8
BM			237	240	244	251	232	239	245	240	6.1

Comparing the hardness profile, it is observed that the tests I1 and I3, that performed with the lowest welding energy, presented higher hardness levels; it is attributed to a higher cooling rate due to its lower welding energy. This led to the appearance of a higher percentage of microconstituents of greater hardness in the welded joint, compared to the tests I2 and I4. The test I3 presented the highest hardness of all, indicating that the presence of the purge gas also influence the microhardness of the weld joint region; it influenced in the cooling rate and the microstructure as seen in item 3.2. In the CGHAZ, this fact can be explained assuming that the reduction of the bainitic transformation

temperature (Bi) with the increase of the cooling rate, results in finer bainitic ferrite slats and it will increase in Vickers hardness.

4. CONCLUSIONS

• The implant test with the aid of the acoustic emission proved to be effective in detecting the moment of formation and propagation of HC, proving the feasibility and sensitivity of this system in the verification of this type of crack.

• Hydrogen cracking emerged and propagated within a maximum test time of 5 hours.

• It was verified that the formation of HC occurred in the region of coarse grains of the HAZ, which is due to the appearance of microstructures more susceptible to the cracking formed during the cooling.

• The purge gas used influenced the in refinement of the microstructure under the welding conditions tested (I3 and I4).

• The low load inserted in the test I1, in spite of the low welding energy, evidenced the need for a higher load applied, in agreement with the literature; so that there is cracking and /or rupture of the SM.

• No cracks occurred in the implant. The crack will always occur at the boundary of CGHAZ/FZ due to the presence of high restrictions, crack propagation time, residual hydrogen from welding, susceptible microstructure and the amount of carbon equivalent of the material being in the range of susceptible materials.

5. ACKNOWLEDGEMENTS

To CAPES for funding this research with scholarship.
To the PPGEM / DMM of the Federal Institute of Maranhão/ IFMA for the support to the development of this scientific pape.
To the LTPSolda by the realization of the tests.

6. REFERENCES

Aquino, A. F. “Estudo do Comportamento Mecânico de Juntas do Aço API 5L X80 Soldadas com Arames Tubulares Undermatched e Evenmatched". 2011. 84f. Tese (Doutorado em Engenharia Mecânica)- Universidade Federal de Pernambuco, Recife, 2011.

Bezerra, A. A. “Trinca a Frio na Soldagem”. Sinergia, São Paulo, v.6, n.1, p.71-76, jan./jun. 2005.

Boellinghaus,T., Viyanit, E., Zimmer, P. 2010. “Cold Cracking Tests”. Revision, IIW – Doc. Nº II-A- 111.03-Revision6. 03 August 2016 <http://www.china-weldnet.com/English/information/II-1587-06.htm>.

Fals, H. C; Trevisan, R.E. “Uso del Ensayo de Implante y la Técnica de Emisión Acústica para Estudiar el Agrietamiento Asistido por Hidrógeno em la Zona Fundida en la Soldadura de un Acero HSLA-80”. Rev. Metal. Madrid, 35 (4), 1999.

Ferraresi, V. A. “Estudo do fenômeno Trinca de Reaquecimento com auxílio da Emissão Acústica”. 1996.173 p. Tese (Doutorado em Engenharia Mecânica), Universidade Estadual de Campinas, Campinas, SP. 1996.

Martins, W.P. “Utilização da Técnica de Emissão Acústica no Estudo da Trinca de Hidrogênio na Soldagem de um Aço de Alta Resistência”. 167f. Tese (Doutorado em Engenharia Mecânica)- Universidade Federal de Uberlândia, Uberlândia. 2013.

Nevasmaa, P. “Predictive model for the prevention of weld metal hydrogen cracking in high-strength multipass welds”. Department of Mechanical Engineering, University of Oulu, P.O.Box 4200, FIN-90014 University of Oulu, Finland Oulu, Finland, 2003.

Pereira, A.S. et al. “Soldagem em Operação de Dutos de Alta Resistência e Baixa Espessura com Ênfase nas Trincas a Frio”. Soldag. Insp. São Paulo, Vol.17, Nº. 2, p.088-095, Abr/Jun 2012.

Ramirez, M.G. et al. “Caracterização Microestrutural de um Aço API 5L-X80 através de Microdureza e Microscopia Ótica e Eletrônica”. In: 62º Congresso Anual da ABM / 62nd ABM International Annual Congress, Vitória – Es. 2007.

Silva, H. R., Ferraresi, V. A. ”Estudo dos Métodos de Determinação da Sensibilidade ao Trincamento à Frio em Juntas Soldadas”. 2006. 16º POSMEC. UFU. Uberlândia. 2006.

Soeiro, J. C.; Rocha, D. B.; Brandi, S. D. "Uma Breve Revisão Histórica do Desenvolvimento da Soldagem dos Aços API para Tubulações". Soldagem & Inspecao, v. 18, n. 2, p. 176–195, 2013.

7. RESPONSIBILITY NOTICE

The authors are the only responsible for the printed material included in this paper.